Preparation and Characterization of Bimetallic Cu-Ni and/or Ni-Cu core-shell Nanoparticles with High Photocatalytic Activity

Rarm Phinjaroenphan[1]*, Kornkanok Boonserm[2] and Surachet Rattanasuporn[3]

[1]Department of Applied Physics, Faculty of Sciences and Liberal Arts, Rajamangala University of Technology Isan, Nakhon Ratchasima, 30000, Thailand

[2]Department of Applied Chemistry, Faculty of Sciences and Liberal Arts, Rajamangala University of Technology Isan, Nakhon Ratchasima, 30000, Thailand

[3]Synchrotron Light Research Institute (Public Organization), Nakhon Ratchasima 30000, Thailand

* Corresponding author. E-mail address: rarm.phin@gmail.com

Received: 9 July 2020; Revised: 8 September 2020; Accepted: 16 September 2020

Abstract

One-pot synthesis of bimetallic Cu-Ni and/or Ni-Cu core-shell nanoparticles have been synthesized by aqueous reduction process, which was very simple, convenient, and prepared under ambient condition. The core-shell system of Cu and Ni could be formed by injecting copper nitrate into an aqueous mixed solution that contained sodium citrate, nickel sulfate, and sodium borohydride. In addition, the injecting time of copper nitrate has a huge effect to obtained either Cu-Ni or Ni-Cu core-shell products with various in size of core and shell structures. Hence, in this report, we explored the morphology and structural information of Cu-Ni and/or Ni-Cu core-shell nanoparticles with varied injecting time of copper nitrate such as 1 min, 5 min, and 10 min, respectively. The effect of the copper nitrate injecting time on the nanoparticles size and types of core and shell also investigated. The bimetallic products were characterized by X-ray diffraction (XRD), high resolution transmission electron microscopy (HR-TEM), and Energy Dispersive X-ray Spectrometer (EDS) methods. Beside, we provided information of photocatalytic activity under UV light illumination of the bimetallic nanoparticles. Compared with Ni monometallic nanoparticle, the bimetallic products enhanced the photocatalytic activity.

Keywords: Cu-Ni and/or Ni-Cu core-shell nanoparticles, Ni nanoparticles, bimetallic nanoparticles, aqueous reduction process, photocatalytic activity

Introduction

Bimetallic nanoparticles derive much attention from many researchers because of their important applications in nanoscience. These particles have been known as a combination of two different metals that at least one of them has a structure in nanoscale. Since the presence and complex of two different metal compositions, bimetallic nanoparticles often show higher physical and chemical properties compare with monometallic nanoparticles. For this reason, they have been used with potential application in various field, such as catalysis (Lim et al., 2009; Huber, Shabaker, & Dumesic, 2003; Ibrahim, Hayyan, AlSaadi, Hayyan, & Ibrahim, 2016), electrochemistry (Murray, 2008; Bing, Liu, Zhang, Ghosh, & Zhang, 2010), magnetism (Sun, Murray, Weller, Folks, & Moser, 2000; Song et al., 2009), and optics (Yan et al., 2012; Fu, Kho, Dinish, Koh, & Malini, 2012), respectively.

Bimetallic nanoparticles have complicated and unique structures that can be recognized in different forms, such as alloys, core-shell, and contact aggregate (Gilroy, Ruditskiy, Peng, Qin, & Xia, 2016). Since the size, shape, and metal compositions are important parameters to control or even enhance the chemical, optical, electrical, and catalysis properties of bimetallic nanoparticles (Gilroy et al., 2016; Srinoi, Chen, Vittur, Marquez, & Lee, 2018). To explore and/or develop the nanoparticles with capable of physical and chemical

properties as well as specific potential applications, it is necessary to understand, control, or/and improve morphology of the nanoparticles. Hence, the technique that can control precisely of their morphology is needed and essential. Recently, Carroll et al. (2010) successfully fabricated Ag-Fe and Fe-Ag core-shell nanoparticles by aqueous reduction. They showed that the morphology as well as type of the core-shell nanoparticles could be control by changing the time of adding $AgNO_3$ into the Fe precursor solution.

Among the widely application of bimetallic nanoparticles, their potential utilize as a catalyst for eliminating of hazard dye effluents from industrials, such as paints, textiles, printing inks, and papers, have been received much attention. The degradation of organic dye procedure begins with activate the suitable bimetallic nanoparticles in aqueous solution by sunlight to have highly redox activity. Then, both the oxidation and reduction reactions due to catalyst occur in order to remove and complete degrade dye. After the first reported of using bimetallic nanoparticles for removal of water pollutants in 1970 (Fowkes, Anderson, & Berger, 1970), many researches on the removal of dye for water treatments by various bimetallic nanoparticles have been rapidly increased. Moreover, most of them pointed out that the photocatalytic activity of bimetallic products have been improved and enhanced when compare with monometallic nanoparticles (Tee, Bachas, & Bhattacharyya, 2009; Albonetti et al., 2008; Liu, Jackson, & Eichhorn, 2011; Barakat, Al-Hutailah, Hashim, Qayyum, & Kuhn, 2013).

Although the bimetallic nanoparticles that comprising of Cu and Ni have been recently received interest due to high performance catalysts (Ahmed, Ramanujachary, & Lofland, 2008) and large magnetoresistance properties (Akbulut & Inal, 1998), there is a few report on the investigation of Cu-Ni nanocomposite. Hashemizadeh and Biglari (2018) prepared Cu-Ni nanoparticles by simple hydrothermal method. They reported that the synthesized Cu-Ni nanoparticles is not only appropriate for use as magnetic heterogeneous catalyst, but also use as photocatalysis activity for eliminate methylene blue and methyl orange. Mohamed Saeed, Radiman, Gasaymeh, Lim, and Huang (2018) obtained Ni-Cu nanoparticles via a mild hydrothermal process. The fabricated Ni-Cu nanoalloy was founded to be paramagnetism and their saturation magnetization decreased with increased Ni concentration. Yamauchi et al. (2010) also investigated Cu-Ni nanoparticles with various composition of Cu and Ni by intramolecular reduction of formate complexes of copper (Cu^{2+}) and nickel (Ni^{2+}) under microwave irradiation. They observed oxidation characteristics and the magnetic properties and presented that the molar ratios of Cu and Ni have significantly effect on the magnetic properties of Cu-Ni nanoparticles.

In this work, we presented the one-pot synthesized Cu-Ni and/or Ni-Cu core-shell nanoparticles via simultaneous reduction process preforming under ambient conditions. This research not only proposed the simple, economical, non-toxic, free to use of specialized instruments. But it also demonstrated the simply process to control desired core and shell type as well as their morphological formation. The core-shell nanoparticles were synthesized by injecting copper nitrate into an aqueous solution that contained sodium citrate, nickel sulfate, and sodium borohydride. In addition, the injecting time of copper nitrate after sodium borohydride would played an important role to determine either Cu-Ni or Ni-Cu core-shell products with various in size of core and shell structures. Therefore, we investigated and discussed the effects of copper nitrate injecting time on the nanoparticle size as well as core and shell types.

Moreover, the photocatalytic ability for removal of a toxic dye such as methyl orange under UV light illumination of the prepared Cu-Ni or Ni-Cu nanoparticles has been examined and compare with Ni nanoparticles.

Methods and Materials

Sample preparation

All chemical reagents are received in analytical grade and used without any further purification. Copper nitrate ($Cu(NO_3)_2.3H_2O$), trisodium citrate dehydrate ($Na_3C_6H_5O_7.2H_2O$), nickel sulfate heptahydrate ($NiSO_4.6H_2O$), sodium borohydride ($NaBH_4$), and methyl orange are purchased from Sigma Aldrich.

Synthesis of Ni and Cu-Ni core-shell nanoparticles

The preparation process of Ni nanoparticles can be explained briefly as the following procedure. 0.46 mM trisodium citrate and 4.6 mM nickel sulfate were combined into 100 mL distilled water under constant stirring at room temperature. During stirring, 8.8 mM sodium borohydride was added and the color of mixture solution was changed from clear to a dark gray and black, which indicated that Ni particles were formed. The solution was stirred for another 10 min to make a complete reaction. The resulting solution was quenched with ethanol several times. After that, the precipitation of Ni nanoparticles were obtained by using a centrifuge and washed with distilled water. The particles were dried in a vacuum oven at room temperature.

The synthesis process of Cu-Ni/Ni-Cu core-shell nanoparticles were quite similar to the preparation of Ni, but the difference was the presence of copper. In this process, the adding time of copper nitrate is an important parameter that has significantly effect on core and shell type as well as structures of the nanoparticles. To fabricate Cu-Ni/Ni-Cu core-shell formations, 0.5 M $Cu(NO_3)_2$ solution needed to be prepared as a stock solutions. After preparing the mixture solution that contained trisodium citrate, nickel sulfate, distilled water, and sodium borohydride with the same concentration as above mention, the $Cu(NO_3)_2$ precursor is injected into the mixture solution for the desired time at 1 min, 5 min, and 10 min, respectively.

Characterization

The X-ray diffraction (XRD) measurements were carried out using a Rigaku D/Max 2500 X-ray diffractometer with CuK_α radiation of wavelength 0.154 nm. The high resolution TEM images were recorded with a Tecnai G2 20 transmission electron microscopy (HR-TEM). The TEM samples were prepared by dropping the solution over the copper grids and allowing the solvent to evaporate in the vacuum chamber at 25 ^{o}C. The energy dispersion X-ray spectrometer (EDS) type attached to the scanning electron microscopy (SEM) was performed. The SEM samples were prepared by placing nanoparticles after evaporated in the vacuum chamber over the carbon tape.

Photocatalytic activity evaluation

The photocatalytic activity of the nanoparticle samples was evaluated in term of the degradation rates of methyl orange (MO) by UV-Vis spectrophotometer. For 0.2 g of each sample was dispersed in 50 mL of 10 ppm of MO in aqueous solution. The mixture solution was stirred for 30 min in the dark, then irradiated under UV light with a 300-W high-pressure Hg lamp working as a UV light source. At every 30 min for UV irradiation time, 5 mL of the suspended solution was taken, centrifuged, and filtered. The photocatalytic activity was evaluated by checking the MO concentration of the filtrate with a UV-Vis spectrometer at 463.8 nm (This wavelength corresponding to MO maximum absorption).

Results and Discussions

The crystal phase of the nanoparticle products were identified by XRD analyzed as shown in Figure 1. The diffraction peaks of Ni nanoparticles were observed at $2\theta = 44.40^{\circ}$ and 51.80°, corresponding to reflection plane (111) and (200) of face center cubic (fcc) Ni metal, according to JCDS file no.4-0850, respectively. In addition, there was no observed impurity oxides peaks, suggested that NiO, NiO_2, or Ni_2O_3 phases did not obtained in the particles.

The XRD profiles of Cu-Ni nanoparticles were similar regardless of various $Cu(NO_3)_2$ time adding. The diffraction patterns showed two double peaks, which could be extracted each diffraction peaks at $2\theta = 43.30^{\circ}$, 44.40°, 50.43°, and 51.80°, respectively. These peaks were also matched with the characteristic peaks from both fcc Cu ($2\theta = 43.30^{\circ}$ (111), 50.43° (200), according to JCDS file no.4-0836) and Ni metals ($2\theta = 44.40^{\circ}$ (111), 51.80° (200)), which suggested the co-existence of Cu and Ni phases. These patterns were clean, leading to be no impurity oxide phase occurred.

Morphology and structural information of the nanoparticles were observed with HR-TEM, as shown in Figure 2. The Ni nanostructure was obtained in a spherical formation with approximately 15.78 nm, as indicated in Figure 2a. The observed bimetallic structures of the Cu-Ni nanoparticles were very interested as they changed significantly depend on the time of adding $Cu(NO_3)_2$. In particular, the core-shell system was formed in case of the adding time of $Cu(NO_3)_2$ at 1 (Cu-Ni 1) and 5 min (Cu-Ni 5) as shown in Figure 2b, c. The particle size of Cu-Ni 1 was observed about 20.23 nm (14.45 nm of core size and 2.89 nm of shell thickness), which was slightly smaller than that value of Cu-Ni 5, around 21.98 nm (16.54 nm of core size and 2.72 nm of shell thickness). While the cluster core with small island overgrowth was revealed at 10 min of the adding time of $Cu(NO_3)_2$, as indicated in Figure 2d. The core cluster size were obtained more than 180 nm. All the structural information are summarized and shown in Table 1.

To gain more details of the nanoparticles morphology, the EDS measurements are essential. Since the particles contained Cu, the carbon adhesive tapes was used to support the samples during the measurements. These studies not only confirmed the presence of Cu and Ni, but also evaluated their atomic percentage of the samples surface. The atomic number of Ni was observed higher for Cu-Ni 1 (72.5%) and slightly higher for Cu-Ni 10 (54.4%), but lower for Cu-Ni 5 (19.8%) than that value of Cu, which was 27.5, 80.2, and 45.6% for Cu-Ni 1, Cu-Ni 5, and Cu-Ni 10, respectively. These suggested that Cu core with Ni shell appeared when $Cu(NO_3)_2$ injecting time is 1 min, but Ni core with Cu shell are formed instead if the injecting time is 5 min. Moreover, if we added $Cu(NO_3)_2$ after 10 min, the Ni core cluster attached with small Cu islanding are obtained. Beside, only Ni component is presence in the Ni samples, confirmed that Ni monometallic nanoparticles were formed. The metal compositions of the synthesized nanoparticles were also listed in Table 1.

The above results indicated that the different in morphology of the derived particles depended much on the time of injecting $Cu(NO_3)_2$ into the mixture solution (trisodium citrate, nickel sulfate, and $NaBH_4$). Figure 3 depicted the formation mechanism of developed Cu-Ni/Ni-Cu core-shell and Ni nanoparticles, which could be explained base on the discrepancy of reduction potential in an aqueous solution. Since the reduction potential of Ni^{2+} to Ni and Cu^{2+} to Cu is -0.25 V and 0.34 V, respectively (Gilroy et al., 2016), the reduction of Ni required a slightly longer time than that of Cu. For the 1 min of addition $Cu(NO_3)_2$, Cu could grow and formed faster, then behaved as a nucleation center for the Ni to grow around, lastly, became to Cu core and Ni shell

nanoparticles. When the injecting time was prolonged to 5 min, Ni might have enough time to form and act as a nucleation site instead, then followed by Cu to grow, consequently, Ni-Cu core-shell nanoparticles was fabricated. Then, if the injecting time was prolonged longer, as 10 min, large Ni cluster core were created and attached with small Cu overgrowth as islanding.

The photocatalytic performance of the synthesized nanoparticles were evaluated by examining the degradation rate of methyl orange (MO) under UV light irradiation at various time, as shown in Figure 4. It was revealed that, after 120 min, more than 90% of MO was degraded by bimetallic Cu-Ni 1 and Cu-Ni 5 nanoparticles, as shown in figure 4b and 4c. While about 81.6% and 79.2% of MO were eliminated by monometallic Ni (figure 4a) and bimetallic Cu-Ni 10 nanoparticles (figure 4d), respectively.

The obtained photocatalytic rate indicated that the bimetallic nanoparticles exhibited higher and enhanced as it was expected due to the intermetallic effects between Cu and Ni. However, only the Cu-Ni 10 showed lower of degradation rate than the Ni, as it might be due to agglomerate of particles size. Moreover, the Cu-Ni core-shell nanoparticles possessed the best catalysis activity among all the prepared nanoparticles. The reasons for high photocatalytic activity of the Cu-Ni 1 may be contribute to the reduction of charge barrier. Therefore, it increased charge generation and separation of photo-generated hole and photo-generated electron, also prevented their charge recombination (Deng et al., 2009).

Table 1 Nanostructural parameters and metal surface composition of Ni and Cu-Ni/Ni-Cu core-shell nanoparticles prepared at different times of adding $Cu(NO_3)_2$ such as 1 min (Cu-Ni 1), 5 min (Cu-Ni 5), and (Cu-Ni 10) 10 min

Sample	Nanostructure (observed)[a]	Particles size (nm)[a]	Diameter core size (nm)[a]	Shell thickness (nm)[a]	Metal surface composition[b]	
					Cu (Atomic %)	Ni (Atomic %)
Ni	Spherical	15.78±1.53	-	-	-	100
Cu-Ni 1	Cu core-Ni shell	20.23± 2.70	14.45± 2.11	2.89	27.5	72.5
Cu-Ni 5	Ni core-Cu shell	21.98± 2.08	16.54± 1.88	2.72	80.2	19.8
Cu-Ni 10	Ni cluster attached with Cu islanding	>180	-	-	45.6	54.4

[a]Nanostructure, particles size, diameter core size, and shell thickness were determined by HR-TEM

[b]Metal surface composition was evaluated from EDS attached to the SEM

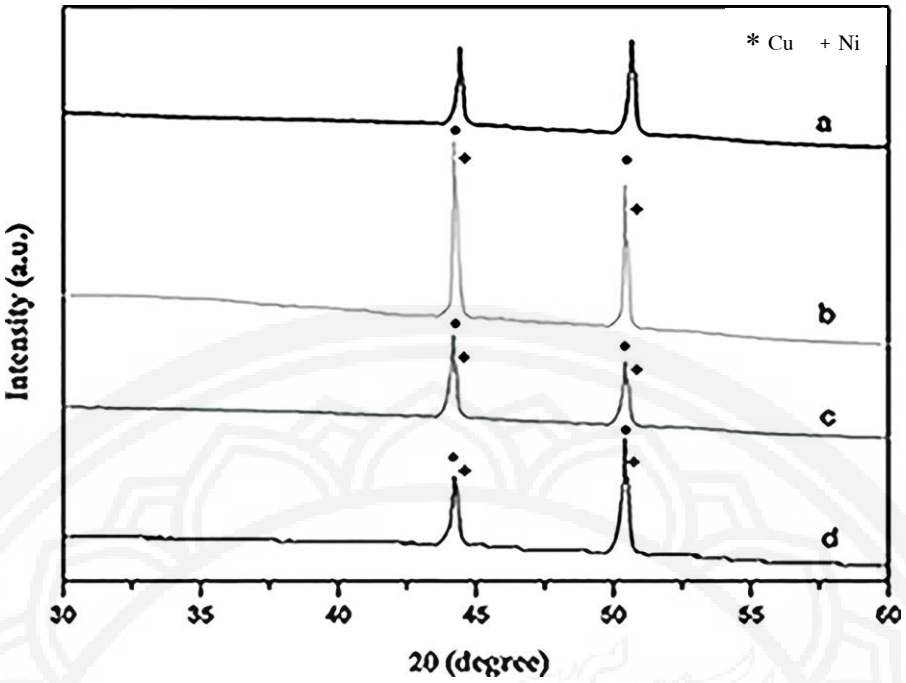

Figure 1 XRD pattern of the synthesized Ni and Cu-Ni/Ni-Cu core-shell nanoparticles by aqueous reduction process; (a) Ni nanoparticles; Cu-Ni/Ni-Cu core-shell prepared at different times of adding $Cu(NO_3)_2$; (b) 1 min; (c) 5 min; (d) 10 min (* Cu JCDS file 4-0836 (Cu) + Ni JCDS file 4-0850 (Ni))

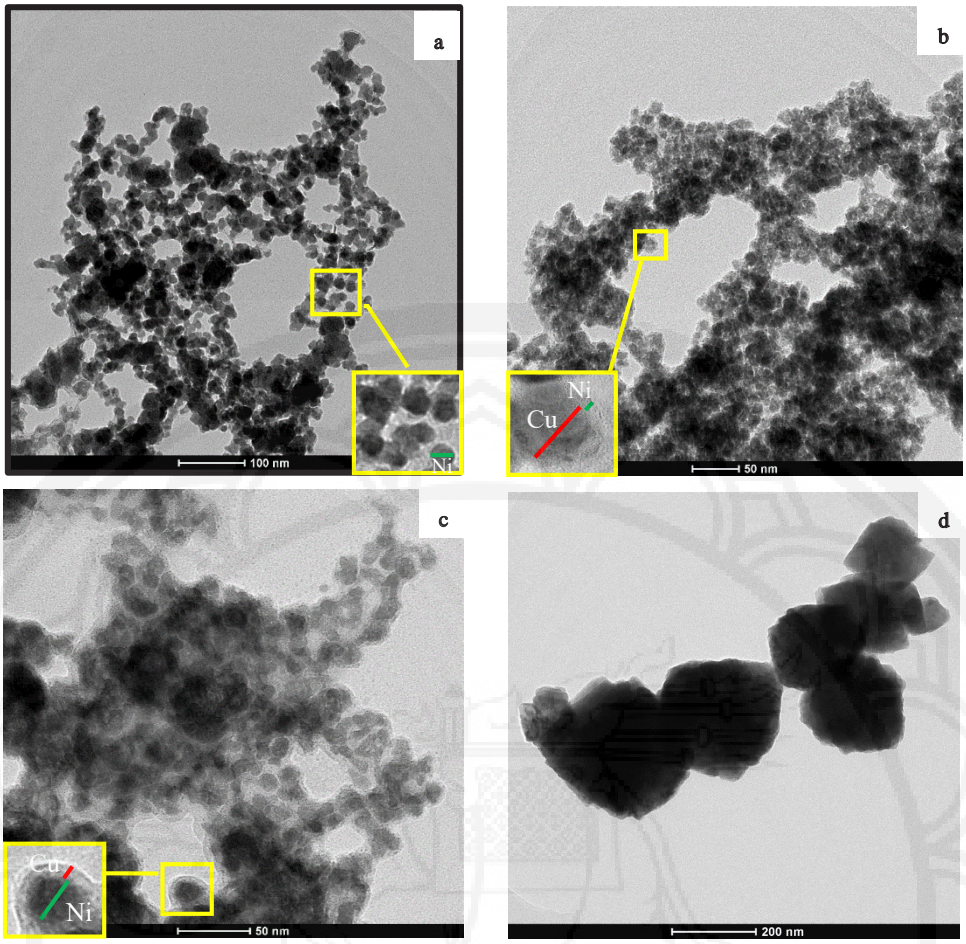

Figure 2 High resolution TEM images of the synthesized Ni and Cu-Ni/Ni-Cu core-shell nanoparticles by aqueous reduction process; (a) Ni nanoparticles; Cu-Ni/Ni-Cu core-shell prepared at different times of adding $Cu(NO_3)_2$; (b) 1 min; (c) 5 min; (d) 10 min

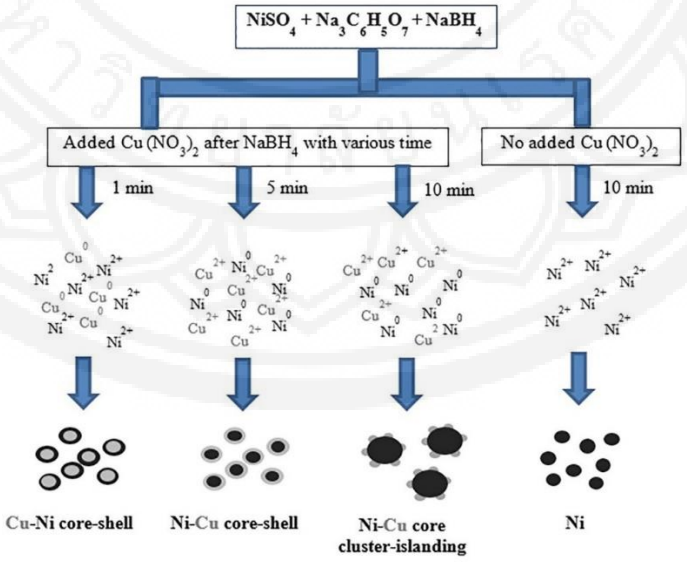

Figure 3 Schematic representation of the formation mechanism of the synthesized Ni nanoparticles and Cu-Ni or Ni-Cu core-shell nanoparticles at different times of injecting $Cu(NO_3)_2$ (1, 5 and 10 min) into the mixture solution; trisodium citrate, nickel sulfate, and $NaBH_4$

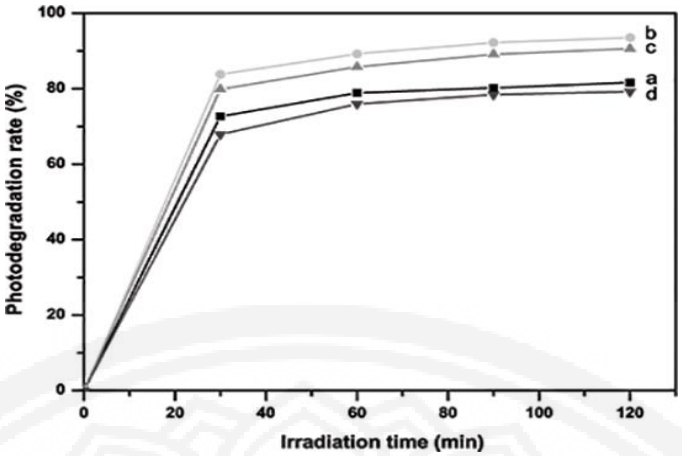

Figure 4 Photodegradation rate of MO under UV light irradiation by the synthesized monometallic Ni and bimetallic Cu-Ni/Ni-Cu core-shell nanoparticles; (a) monometallic Ni nanoparticles ; bimetallic Cu-Ni and Ni-Cu core-shell nanoparticles prepared at different times of adding $Cu(NO_3)_2$; (b) 1 min (Cu-Ni 1); (c) 5 min (Cu-Ni 5); (d) 10 min (Cu-Ni 10)

Conclusion and Suggestions

We have been successfully produced Cu-Ni and/or Ni-Cu core-shell and Ni nanoparticles using a simply one-pot aqueous reduction method. This synthesis mechanism is very convenient, economical, not need specialized instruments, perform under ambient condition, and using only one parameter to control desired morphology as well as core and shell type of the nanoparticles. The Cu-Ni and Ni-Cu nanoparticles were obtained by adding the $Cu(NO_3)_2$ into the previous mixture aqueous solution (trisodium citrate, nickel sulfate, and $NaBH_4$). The time of injecting $Cu(NO_3)_2$ after $NaBH_4$ played an important role on the controlling of structure of the bimetallic products.

For example, Cu core and Ni shell nanoparticles were formed when the injecting time of $Cu(NO_3)_2$ is 1 min. However, if the injecting time increased to 5 min, Ni core and Cu shell having slightly bigger size were formed instead. Lastly, if the injecting time increased further to 10 min, large Ni core cluster attached with small Cu overgrowth as islanding were observed. While, Ni nanoparticles were derived from the mixture solution without adding $Cu(NO_3)_2$.

Moreover, the synthesized nanoparticles showed highly efficient in the elimination of methyl orange under UV light illumination. The degradation ability of the bimetallic products were improved compare to the monometallic due to the synergetic effect of Cu and Ni. Experimental results also showed that the Cu-Ni core-shell nanoparticles achieved the highest photocatalytic activity, which capable to degrade methyl orange about 93.5% within 120 min.

References

Ahmed, J., Ramanujachary, K. V., & Lofland, S. E. (2008). Bimetallic Cu-Ni nanoparticles of varying composition ($CuNi_3$, CuNi, Cu_3Ni). *Colloids and Surfaces A*, *331*, 206-212.

Albonetti, S., Bonelli, R., Mengou, J. E., Femoni, C., Tiozzo, C., Zacchini, S., & Trifirò, F. (2008). Gold/iron carbonyl clusters as precursors for TiO_2 supported catalysts. *Catalysis Today, 137*, 483-488.

Akbulut, H., & Inal, O. T. (1998). Plasma-assisted deposition of metal and metal oxide coatings. *Journal of Materials Science, 33*, 1189-1199.

Barakat, M., Al-Hutailah, R. l., Hashim, M. H., Qayyum, E., & Kuhn, J. N. (2013). Titania-supported silver-based bimetallic nanoparticles as photocatalysts. *Environmental Science and Pollution Research, 20*, 3751-3759.

Bing, Y., Liu, H., Zhang, L., Ghosh, D., & Zhang, J. (2010). Nanostructured Pt-alloy electrocatalysts for PEM fuel cell oxygen reduction reaction. *Chemical Society Reviews, 39*, 2184-2202.

Carroll, K. J, Hudgins, D. M., Spurgeon, S., Kemner, K. M., Mishra, B., Boyanov, M. I., Carpenter, E. E. (2010). One-pot aqueous synthesis of Fe and Ag core/shell nanoparticles. *Chemistry of Materials, 22*, 6291-6296.

Deng, L., Wang, S., Liu, D., Zhu, B., Huang, W., Wu, S., & Zhang, S. (2009). Synthesis, characterization of Fe-doped TiO_2 nanotubes with high photocatalytic activity. *Catalysis Letters, 129*, 513-518.

Fowkes, F. M., Anderson, F. W., & Berger, J. E. (1970). Bimetallic coalescers: electrophoretic coalescence of emulsions in beds of mixed-metal granules. *Environmental Science and Technology, 4*, 510-514.

Fu, C. Y., Kho, K. W., Dinish, U. S., Koh, Z. Y., & Malini, O. (2012). Enhancement in SERS intensity with hierarchical nanostructures by bimetallic deposition approach. *Journal of Raman Spectroscopy, 43*, 977-985.

Gilroy, K. D., Ruditskiy, A., Peng, H.-C., Qin, D., & Xia, Y. (2016). Bimetallic nanocrystals: syntheses, properties, and applications. *Chemical Reviews, 116*, 10414-10472.

Hashemizadeh, S. A., & Biglari, M. (2018). Cu:Ni bimetallic nanoparticles: facile synthesis, characterization and its application in photodegradation of organic dyes. *Journal of Materials Science: Materials in Electronics, 29*, 13025-13031.

Huber, G. W., Shabaker, J. W., & Dumesic, J. A. (2003). Raney Ni-Sn catalyst for H_2 production from biomass-derived hydrocarbons. *Science, 300*, 2075-2077.

Ibrahim, R. K., Hayyan, M., AlSaadi, M. A., Hayyan, A., & Ibrahim, S. (2016). Environmental application of nanotechnology: air, soil, and water. *Environmental Science and Pollution Research, 23*, 13754-13788.

Lim, B., Jiang, M., Camargo, P. H. C., Cho, E. C., Tao, J., Lu, X., & Xia, Y. (2009). Pd-Pt bimetallic nanodendrites with high activity for oxygen reduction. *Science, 324*, 1302-1305.

Liu, Z., Jackson, G. S., & Eichhorn, B. W. (2011). Tuning the CO-tolerance of Pt-Fe bimetallic nanoparticle electrocatalysts through architectural control. *Energy and Environmental Science, 4*, 1900.

Mohamed Saeed, G. H., Radiman, S., Gasaymeh, S. S., Lim, H. N., & Huang, N. M. (2010). Mild hydrothermal synthesis of Ni-Cu Nanoparticles. *Journal of Nanomaterials, 184137*, 1-5.

Murray, R. W. (2008). Nanoelectrochemistry: metal nanoparticles, nanoelectrodes, and nanopores. *Chemical Reviews, 108*, 2688-2720.

Song, H. M., Kim, W. S., Lee, Y. B., Hong, J. H., Lee, H. G., & Hur, N. H. (2009). Chemically ordered $FePt_3$ nanoparticles synthesized by a bimetallic precursor and their magnetic transitions. *Journal of Materials Chemistry, 19,* 3677-3681.

Srinoi, P., Chen, Y. T., Vittur, V., Marquez, M. D., & Lee, T. R. (2018). Bimetallic nanoparticles: enhanced magnetic and optical properties for emerging biological applications. *Applied Science, 8*, 1-32.

Sun, S., Murray, C. B., Weller, D., Folks, L., & Moser, A. (2000). Monodisperse FePt nanoparticles and ferromagnetic FePt nanocrystal superlattices. *Science, 287*, 1989-1992.

Tee, Y.-H., Bachas, L., & Bhattacharyya, D. (2009). Degradation of trichloroethylene by Iron-based bimetallic nanoparticles. *Journal of Physical Chemistry C, 113*, 9454-9464.

Yamauchi, T., Tsukahara, Y., Sakata, T., Mori, H., Yanagida, T., Kawai, T., & Wada, Y. (2010). Magnetic Cu-Ni (core-shell) nanoparticles in a one-pot reaction under microwave irradiation. *Nanoscale, 2*, 515-523.

Yan, M., Zhang, M., Ge, S., Yu, J., Li, M., Huang, J., & Liu, S. (2012). Ultrasensitive electrochemiluminescence detection of DNA based on nanoporous gold electrode and PdCu@carbon nanocrystal composites as labels. *Analyst, 137*, 3314-3320.